

Conf-9509196--1

UCRL-JC-120091
PREPRINT

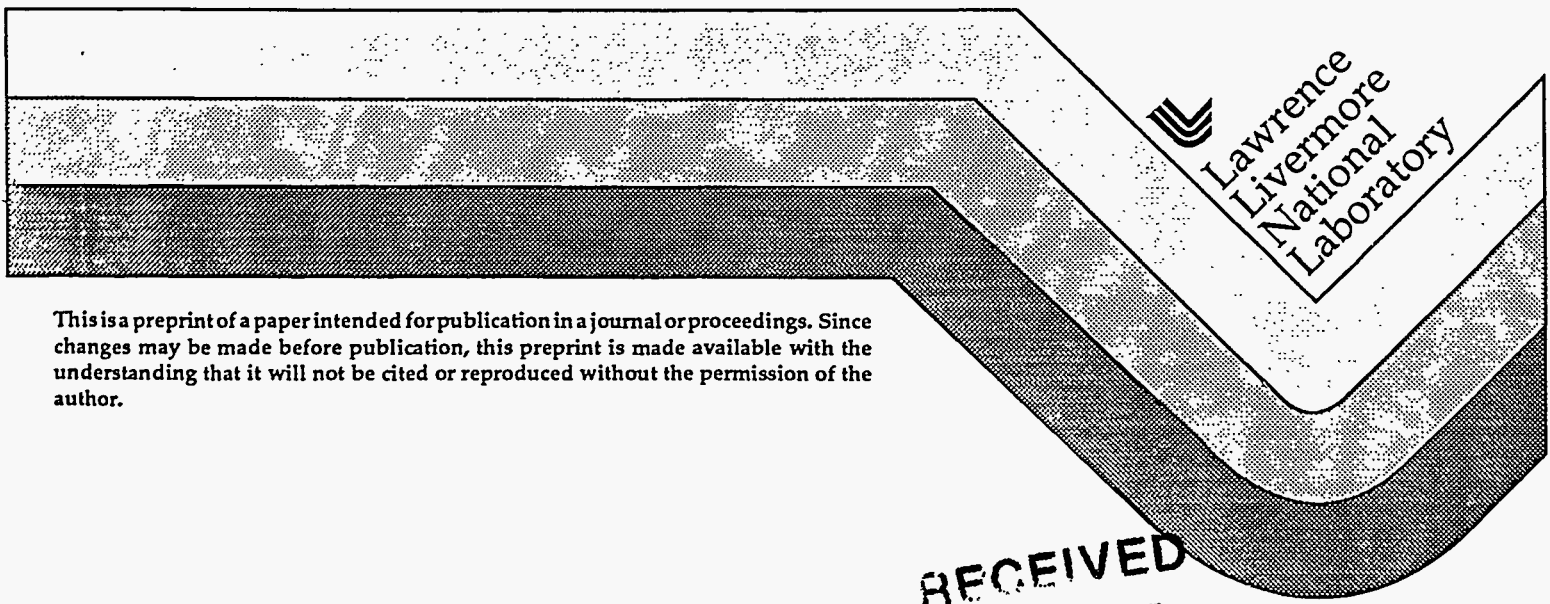
Progress Toward an Optimized Hydrogen Series Hybrid Engine

J. Ray Smith and Salvador M. Aceves

Norman L. Johnson and Anthony A. Amsden
Los Alamos National Laboratory

This paper was prepared for submittal to the
American Society of Mechanical Engineers'
Internal Combustion Engine '95 Fall Conference
Milwaukee, WI
September 24-27, 1995

June 1995



This is a preprint of a paper intended for publication in a journal or proceedings. Since changes may be made before publication, this preprint is made available with the understanding that it will not be cited or reproduced without the permission of the author.

RECEIVED
AUG 04 1995
OSTI

PROGRESS TOWARD AN OPTIMIZED HYDROGEN SERIES HYBRID ENGINE

J. Ray Smith and Salvador M. Aceves
Lawrence Livermore National Laboratory
Livermore, CA

Norman L. Johnson and Anthony A. Amsden
Los Alamos National Laboratory
Los Alamos, NM

ABSTRACT

The design considerations and computational fluid dynamics (CFD) modeling of a high efficiency, low emissions, hydrogen-fueled engine for use as the prime mover of a series hybrid automobile is described. The series hybrid automobile uses the engine to generate electrical energy via a lightweight generator, the electrical energy is stored in a power peaking device (like a flywheel or ultracapacitor) and used as required to meet the tractive drive requirements (plus accessory loads) through an electrical motor. The engine/generator is stopped whenever the energy storage device is fully charged. Engine power output required was determined with a vehicle simulation code to be 15 to 20 kW steady state with peak output of 40 to 45 kW for hill climb. Combustion chamber and engine geometry were determined from a critical review of the hydrogen engine experiments in the literature combined with a simplified global engine model. Hydrogen's high effective octane number and high flame speed permits high compression ratio and very lean operation to simultaneously achieve high efficiency and low NO_x emissions. The baseline design has dual-ignition, 15:1 compression ratio and operates in the 0.4 to 0.5 equivalence ratio range using homogeneous charge. The engine is currently envisioned as naturally aspirated with tuned intake and exhaust at the 15 to 20kW level and supercharged to achieve the 40 to 45 kW power level. The engine is projected to operate in the 1800 to 3600 RPM range to minimize friction losses.

Two different engine models are employed to guide engine design. The models are a simplified global engine performance model that relies strongly on correlations with literature data for heat transfer and friction losses, and a state-of-the-art CFD combustion model, KIVA-3, to elucidate fluid mechanics and

combustion details through full three-dimensional modeling. Both intake and exhaust processes as well as hydrogen combustion chemistry and thermal NO_x production are simulated. Ultimately, a comparison between the simulation and experimental results will lead to improved modeling and will give guidance to changes required in the next generation engine to achieve our goal of 45% brake thermal efficiency.

INTRODUCTION

Lawrence Livermore (LLNL), Sandia Livermore (SNL) and Los Alamos National Laboratories (LANL) have a joint project to develop an optimized, hydrogen-fueled engine for series hybrid automobiles. The major divisions of responsibility are: system analysis, engine design and kinetics modeling by LLNL; performance and emission testing, and friction reduction by SNL; computational fluid mechanics and combustion modeling by LANL. This project is a component of the Department of Energy, Office of Utility Technology National Hydrogen Program. We report here on the progress in modeling and engine design.

The current modeling effort is being applied to two engines. The first, known as the Onan engine, is our initial experimental attempt to achieve optimized combustion in a single-cylinder research engine. The second, is a conceptual engine that would meet the requirements of a series hybrid automobile. Details of the Onan engine currently under test at the Combustion Research Facility of Sandia/California can be found in the paper by Van Blarigan (1995). The Onan engine is a converted diesel engine with a modified head containing two valves and two spark plugs. Table 1 summarizes the engine

DISTRIBUTION OF THIS DOCUMENT IS UNLIMITED

ma

MASTER

specifications. The design of the Onan engine is based on the arguments put forth by Smith et al. 1995. The engine design is such that the bulk flow and turbulence are minimized in order to reduce heat transfer losses, thereby increasing the operating efficiency. The engine operates at low fuel equivalence ratios (0.4-0.5) to reduce the combustion temperature and thereby significantly reduce NO_x emissions.

Table 1 Modified Onan Engine Specifications

Bore	82.55 mm
Stroke	92.08 mm
Displacement.....	493.0 cm ³
Geometric compression ratio	14.82
Rings.....	4 (standard Onan diesel ring pack)
Valve pocket volume.....	3.60 cm ³
Spark plug crevice volume.....	1.30 cm ³
Crevice volume above rings.....	0.27 cm ³

ENGINE DESIGN CONSIDERATIONS

Vehicle system analyses (Aceves and Smith, 1995; Ross and Wu, 1995) have established requirements for engines for series hybrid vehicles that have similar performance to today's automobiles and fuel economy approaching the Partnership for a New Generation of Vehicles (PNGV) goal 3 of 34 km/liter (80 mpg). The first requirement is to operate at a relatively low power of 15 to 20 kW in an on-off mode, at a very high brake thermal efficiency (>40%). Average power requirements for typical urban and highway driving are less than 10 kW. The second requirement is to operate at 40 to 45 kW for long hill climbs. Long hill climbs are the condition that requires the maximum sustained power from the engine. Long hill climbs are expected to be a small part of the total driving time for the vehicle, and therefore engine efficiency can be lower at the high power setting without causing a substantial drop in the typical use fuel economy.

Previous experimental research (Oehmichen, 1942; Olsson and Johansson, 1995), as well as a conceptual analysis by one of the authors (Smith, 1994) have indicated engine characteristics that result in high efficiency and low emissions. Some of the required engine characteristics are:

1. Unthrottled operation to minimize pumping losses. This is possible in the series hybrid since the engine is buffered from the drive wheels and has only two operation points. Thus the engine is optimized for wide open throttle (WOT) operation much like a diesel engine.

2. Lean engine operation. Operating the engine very lean increases the $\gamma (=c_p/c_v)$ of the gases inside the cylinder, resulting in an increased efficiency. A lean mixture also burns at a lower temperature, which decreases heat transfer losses and

NO_x formation.

3. Quiescent chamber. A low turbulence combustion chamber reduces heat transfer losses, and therefore increases engine efficiency. This is possible in hydrogen or high hydrogen to natural gas ratio mixtures due to the flame speed being adequate without high turbulence.

4. Low surface area to volume ratio (S/V) at top dead center (TDC). This also results in decreased heat transfer losses. This requirement indicates that it is desirable to use relatively big cylinders with a long stroke, so that the clearance height at TDC is as large as possible. This also implies a small number of cylinders. Again, transient response of this engine is unimportant since it is buffered from the drivetrain by the electrical interface.

5. A high compression ratio. This increases the thermodynamic efficiency of the engine. This requires a high effective octane number fuel.

6. Low mechanical friction with a ring package that minimizes lubricating oil intrusion into the combustion chamber to minimize hydrocarbon and carbon monoxide emissions.

The need for lean operation and high compression ratio in high efficiency engines points to hydrogen (and, to a lesser degree, methane) as the fuel of choice. Hydrogen has a high flame speed and a high effective octane number, which allows very lean operation at high compression ratio. Hydrogen allows operation at such lean mixtures that thermal NO_x generation can be extremely low while the only hydrocarbons and carbon monoxide emissions come from oxidation of lubricating oil that intrudes into the combustion chamber.

Points (4) and (5) above are often considered as conflicting requirements, since the compression ratio in most experimental engines is increased by increasing the piston height, which decreases the clearance height and increases S/V at TDC. Most analyses and experiments therefore indicate that only small gains are achieved by increasing the compression ratio. However, substantial gains in efficiency can be obtained if the compression ratio is increased by keeping a constant clearance height and increasing the stroke. This is illustrated in Figure 1. This figure is a modification of a figure presented by Muranaka et al. 1987. The figure shows indicated thermal efficiency for a stoichiometric gasoline engine as a function of S/V at TDC, for several compression ratios, based on an engine model. As expected, indicated efficiency decreases as S/V increases, due to heat transfer losses. The dashed curves indicate the efficiency of engines of constant displacement and constant stroke (with equal bore and stroke). These curves were derived by reducing the clearance height to increase the compression ratio as in the original paper. The dotted curves show the efficiency of constant displacement engines with a constant clearance height, where the stroke has been increased to increase the compression ratio. Both displacement curves

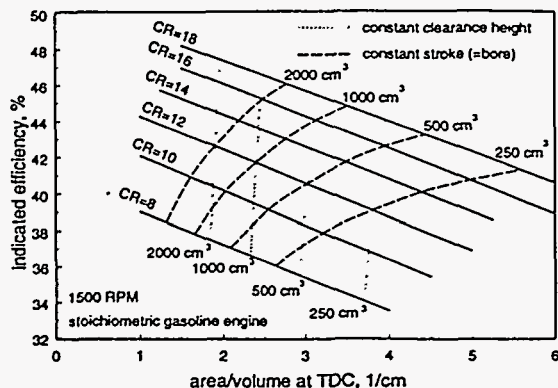


Fig 1 - Indicated thermal efficiency as a function of surface to volume ratio at TDC for various compression ratios and engine displacements with constant stroke (dashed curves) and constant TDC clearance height (dotted curves). Constant clearance height cases have been added to work of Muranaka et al., 1987.

intersect along the CR=12 line, because the constant clearance height for the dotted curves is chosen equal to the clearance height for the dashed lines at CR=12.

Figure 1 shows that, for the constant stroke cases, S/V increases substantially as the compression ratio is increased which results in only a small increase in efficiency as the compression ratio increases. Increasing the compression ratio by increasing the stroke, however, results in only a slight increase in S/V and in a substantial increase in efficiency, as indicated by the constant clearance height cases. It is recognized that a long stroke results in an increased mean piston speed and potentially in added engine friction, but Figure 1 indicates clearly that high compression ratio, long stroke engines should achieve high indicated efficiencies.

A simplified global engine model has been developed to evaluate the design conditions for the next hydrogen engine to be built as a part of this project. This model uses basic thermodynamic relations, and correlations to calculate the specific heats (and therefore γ) for the mixture contained within the cylinder, including residual gases and products of combustion. This model has time dependent heat release but no spatial variation in gas properties. The simplified model does not currently include chemical equilibrium calculations, and assumes no dissociation of the gases. Therefore, this model is expected to be valid only for low equivalence ratio engines, in which the temperatures are relatively low, so that dissociation does not have a major effect on engine efficiency.

The model incorporates a heat loss calculation based on Woschni's model (Woschni, 1967). Woschni's model uses a Nusselt number correlation of $Nu = KRe^{0.8}$ in which the velocity defining the Reynolds number has two contributions. The first contribution is due to the piston motion, and is considered equal to the mean piston speed multiplied by a constant C_1 . The second contribution is due to combustion. Comparing the results of the engine model with the data available for very lean engines, it is clear that the Woschni correlation over predicts heat transfer in lean engines. The reason for this is that Woschni correlation fits typical engines, and the very lean engines analyzed in the literature (and those to be built as a part of this project) have less turbulence and lower temperatures than typical engines. Therefore, we have found it appropriate to use $1/2$ of the original constant C_1 . Other researchers have made similar modifications to the basic Woschni heat transfer correlation (Alkidas and Suh, 1991, Watts and Heywood, 1980). This modification results in reasonable predictions for the long stroke, quiescent chambers studied by Oehmichen, 1942, as illustrated in Figure 2. Figure 3 shows the predictions of this model as compared to the recent experimental data of Olsson and Johansson, 1995, who studied the lean operation of a large engine fueled with natural gas. Olsson and Johansson measured the effect of piston shape on engine efficiency by using different shaped pistons to create varying levels of turbulence in the engine. Their results

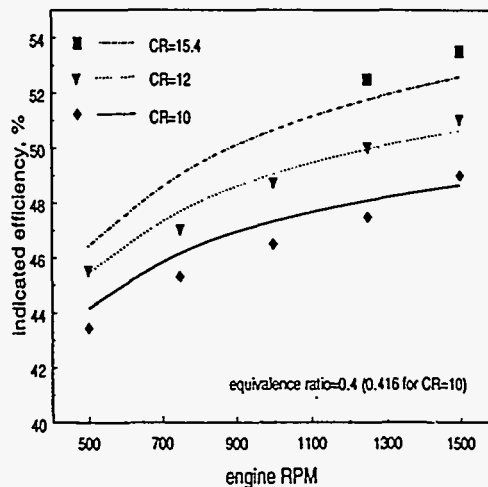


Fig. 2 - Indicated efficiency as a function of engine speed for hydrogen at $\Phi=0.40$. Data points from Oehmichen, 1942, curves from simplified global engine model.

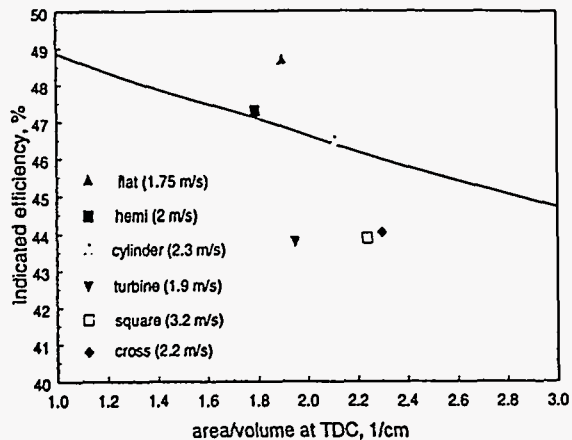


Fig. 3 - Indicated thermal efficiency versus surface to volume ratio. Data points from Olsson and Johansson, 1995, solid curve from simplified global engine model, natural gas fuel at $\Phi=0.625$. Numbers in parentheses indicate average turbulence in the crank angle interval corresponding to 10-90% of heat release.

show that, of the ten pistons compared, a flat top piston had the highest efficiency, due to low S/V and low turbulence. Pistons that generate squish and high turbulence result in increased heat transfer and decreased indicated efficiency. Similar results were reported by Alkidas and Suh, 1991, who varied swirl and tumble by changing inlet valve geometry. Figure 3 shows that, although many of the individual experimental points fall far from the model results, the model predicts reasonably well the efficiency for low to mid turbulence chambers, as well as the general trend of decreasing efficiency as a function of S/V . These data do not correlate well with surface to volume ratio because the turbulence varied enough to cause large differences in burn duration as well. The Woschni correlation has no means to account for combustion chamber shape, and therefore cannot be expected to predict the effect of squish on efficiency. The results in Figures 2 and 3 indicate that the simplified global model developed here can be used as a guide to predict trends. Quantitative results will be validated with the experimental results to be obtained as a part of this project in the near future.

This simplified model has been used as a guide to analyze the next generation engine to be built as a part of this project. To minimize S/V , this engine is expected to have 2 cylinders, with 1.8 liter displacement. The model is used to predict the efficiency at the low power output used for most of the driving

cycle, and also to evaluate the effect of supercharge pressure and increased RPM on engine power output, to verify that the required power output for hill climbing can be obtained within the speed and pressure constraints for the engine.

The simplified engine model was extended to calculate brake power by including correlations for friction losses and supercharger work (for inlet manifold pressure above atmospheric). The correlation for the friction losses as a function of engine speed is obtained from Barnes-Moss, 1975. However, this friction correlation applies to average engines, and it is considered that engines with substantially reduced friction can be built, especially for engines that operate at limited speed and fixed conditions as the one proposed here. Therefore, 65% of the friction losses given by Barnes-Moss' equation are used for the model. Achieving this low friction will require an aggressive friction reduction experimental campaign. Supercharger work calculation assumes a polytropic coefficient of 1.3, and a supercharger mechanical efficiency of 0.9. The model also assumes that an intercooler is used.

The results of this model indicate that the engine will produce slightly over 15 kW of brake power at 1800 RPM and atmospheric manifold pressure. The indicated and brake thermal efficiencies at these conditions are respectively 52% and 45%, comparable to the latest automotive diesels. These conditions appear to be appropriate for the low power conditions used for EPA driving schedules. Figure 4 shows the results of increasing RPM and inlet manifold pressure for obtaining the high power required for long hill climb. The figure shows brake output power as a function of RPM, for different manifold pressures. Based on these results, we propose that the hill climb power can be increased to the required levels (40-45 kW) by a combination of supercharging and increasing the engine RPM. The figure shows that it is necessary to supercharge to 1.75-2 atm while simultaneously increasing engine speed to the 2600-3000 range, to obtain the required power output. Since these values do not result in extreme piston velocities or peak pressure conditions in the engine, it is believed that they can be achieved in a low friction engine that can be used to meet our goal.

ENGINE CFD MODELING

Engine CFD modeling of the Onan hydrogen engine is based on a new version of KIVA-3 with a resolved valve modeling capacity. The valve model allows an analysis of the effects of inlet and exhaust port geometry on engine operating conditions, which have been shown to be important in achieving the high efficiency and low emissions targeted for this project (Alkidas and Suh, 1991).

The KIVA family of codes is a mature, three-dimensional, computational fluid dynamics software for chemically reactive, transient flows with fuel sprays (Amsden et al., 1989). The code features sophisticated sub-models, which simulate the

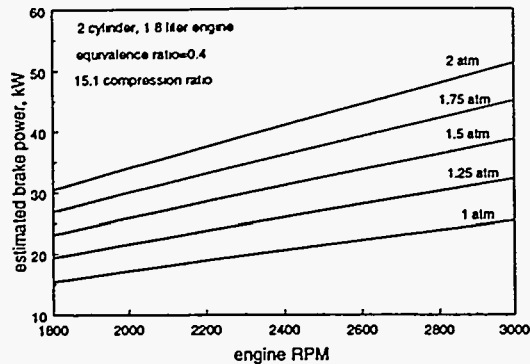


Fig 4 - Estimated brake power as a function of engine speed as a function of inlet manifold pressure based on simplified global engine model at $\Phi=0.40$ for $1,800 \text{ cm}^3$ displacement.

complex flow, thermodynamic and chemical processes accompanying combustion. These models include, for applications to combustion engines: turbulence, spray atomization, fuel penetration and vaporization, auto-ignition and combustion. The chemical combustion model can describe complex equilibrium and kinetic reactions. The KIVA-3 version (Amsden, 1993) enables complex geometries to be modeled, typical of internal combustion engines with moving pistons and inlet and exhaust ports.

Developing the three-dimensional mesh for the Onan engine is a significant undertaking. The mesh resulted from progressive refinements over a period of many months. The final mesh is shown in Fig. 5. The mesh is generated with 41 pseudo-blocks, resulting in 5 logically hexahedral blocks of mesh with 37,722 cells in the full mesh. The setup of the mesh requires the shape of the valves along their path of travel to be included in the initial mesh, as illustrated in Fig. 5. Because the current geometry of the modified Onan engine has a plane of symmetry through the two valves, for the computational results presented here only half of the engine is simulated. The only major simplifications made in the computational mesh were square cross-section of the intake and exhaust manifolds and their reduced length. The flow area of the simulated and actual manifolds are identical. Because the pressure boundary conditions at the intake and exhaust manifolds were expected to be modified in order to obtain agreement with the breathing performance of the engine, the simplification of the length and cross-section of the manifolds is not considered to be significant. Other simplifications are the omission of the crevice volume associated with the spark plugs (3.5% of the minimum cylinder volume) and the crevice volume above the top piston ring (0.7% of the minimum volume). The valve

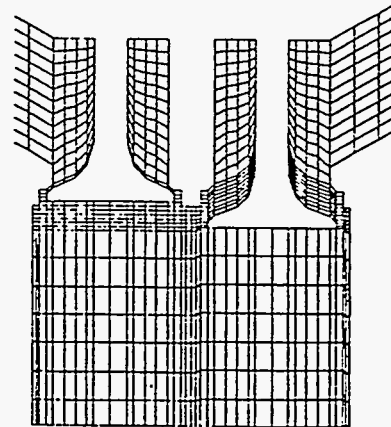
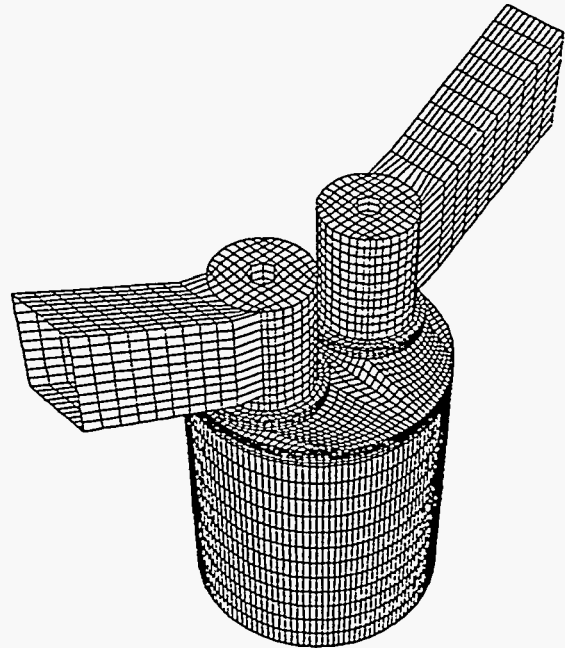


Fig 5 -The mesh for the Onan engine. Perspective view above. Cross-section below showing the inlet valve (right) and the exhaust valve (left).

shapes and seating were modeled accurately to within the resolutions of the mesh.

In the absence of experimental data on the Onan engine for comparison to the KIVA simulation results, a variety of simulations were done to evaluate the performance and sensitivity of the model. Simulations were initialized at just before intake valve opening (20 CA BTDC) and carried through the intake cycle, the closing of the intake valve and compression, and then stopped just before ignition. The state

of the calculation was stored at this time so that the simulation could be continued with a variety of ignition timing and changes in the reactive kinetic models.

The kinetics of hydrogen oxidation were modeled by a single forward kinetic equation, with an Arrhenius temperature dependence. Zeldovich kinetics for the NO_x production are also included. The effect of turbulence on the combustion rate was included by using a mixing controlled combustion model (a slight variation of the model proposed by Magnussen and Hjertager, 1977) in which the reaction rate is proportional to the time scale of the ratio of the turbulent kinetic energy to the rate of dissipation of turbulence, i.e., k/ϵ . The inclusion of the mixing controlled model is essential because the flame speed of the hydrogen combustion is many times the laminar flame speed in the presence of typical turbulent intensities found in engines (Meier et al., 1994). Increases of factors of 25 times the laminar flame speed have been observed for propane (Abdel-Gayed and Bradley, 1976). The present mixing controlled combustion model is applied routinely to hydrocarbon combustion, but has not been applied to hydrogen combustion. Until the model is validated, results using the turbulent mixing combustion model should only be used to examine trends in the simulations.

All the simulations ran without difficulty or unexpected termination. Execution times were about two hours on a Cray YMP to reach the time of ignition, or about 360 degrees of crank angle. Combustion simulations from -20 CA to +20 CA around TDC required about an hour of computational time. All aspects of the simulations associated with the fluid dynamics were reasonable, and we expect them to be predictive of the Onan engine performance.

The only area of difficulty arose in the simulation of combustion of hydrogen. The primary difficulty that was encountered was the autoignition of the hydrogen during compression, when parameters in the single step oxidation kinetics were used which reproduce the laminar flame speed (Westbrook, 1994). Preliminary experimental results (Van Blarigan, 1995) indicate that for these operating conditions, autoignition does not occur. This deficiency of the hydrogen kinetics was also observed in the KIVA simulations of hydrogen injection and combustion (Johnson et al., 1995) by the absence of an autoignition delay. Our solution to the difficulty is similar: enforce that the hydrogen kinetics reproduce the observed behavior by preventing the hydrogen reaction from proceeding until the cell temperature has exceeded 1000K. This approach does not require a modification of KIVA, because a cut-off temperature, typically 800K, is commonly used in which the kinetics will not be calculated if the cell temperature is below this value. The consequence of this approach is to inhibit the reaction as compression of the fuel mixture occurs and enable the reaction at and behind the combustion front, typically at temperatures over 2000K. We

consider this to be a temporary solution until better kinetics are available. In the absence of the higher cutoff temperature, the hydrogen fuel would autoignite when it reached 800K, typically about 10 degrees BTDC for an intake manifold pressure of 1.2 atm, independent of the time of ignition.

Importance of Modeling Induction

In the absence of experimental data to benchmark the performance of KIVA-3 for the Onan engine, we undertook a computational study to evaluate the importance of including the air-fuel induction process prior to combustion. We made two simulations, one with no induction into the cylinder and another with flow through the intake valve and the subsequent generation of bulk flow and turbulence, and then compared the effects on combustion and time histories of flow energies. The simulation with intake flow was accomplished as described in the previous section. The simulation without induction was begun just after intake valve closing and the composition was set to be identical to the simulation with induction at the same crank angle. The bulk flow was specified to be quiescent, and the turbulent kinetic energy per mass was taken to be ten percent of the kinetic energy per mass as obtained from the maximum piston velocity. These are typical starting conditions for a quiescent engine when more detailed information is not known.

In the simulation with air induction, the technique for inhibiting autoignition described in the previous section was used. For the simulation with quiescent starting conditions, the hydrogen mixture would not sustain combustion after ignition using identical kinetics and ignition as the simulation with air induction. The difficulty appeared to be associated with the small heat release of the low fuel equivalence ratio mixture, and not the propagation of the combustion once the mixture was sufficiently enflamed. By doubling the number of cells where the ignition occurred (from 2 cells to 4), increasing the energy deposition used to model the spark by 2.5, and by lowering the cutoff to inhibit the autoignition to 850K from 1000K, the combustion wave was sustained in the simulation.

Figures 6 and 7 show the cylinder-averaged pressure and temperature during the compression, combustion, and expansion part of the cycle, up until the opening of the exhaust valve at 450 CA. As expected, until the time of combustion these curves are identical for both runs. After combustion at 13.5 CA BTDC (346.5 CA in the simulation), there is significant divergence in the two simulations, a difference of 17.5 bars in pressure and 137K in temperature. The major difference in the two simulations is that the flame speed is about 3.5 times larger in the inducted (high turbulence) simulation. The differences in the combustion behavior have a significant impact on the production of NO_x emissions. In Fig. 8 the NO_x production is two times higher in

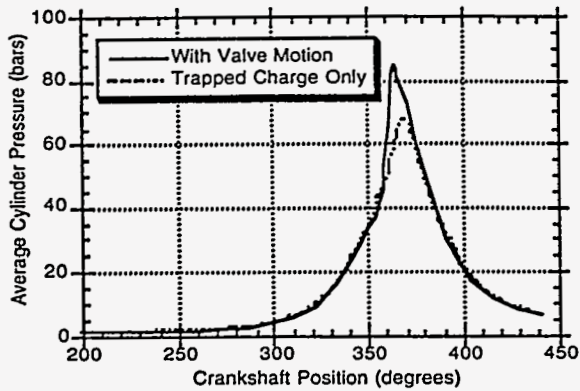


Fig. 6 - Pressure histories averaged over the cylinder after intake valve closing.

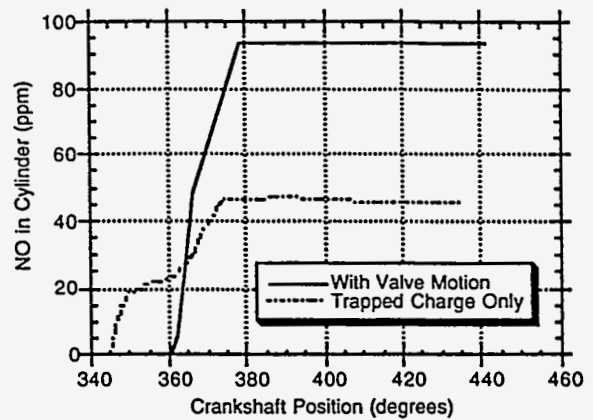


Fig. 8 - NO_x production in the cylinder during combustion.

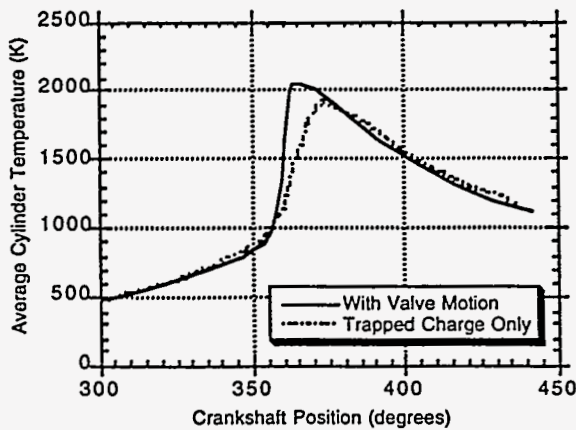


Fig. 7 - Temperature histories averaged over the cylinder after intake valve closing.

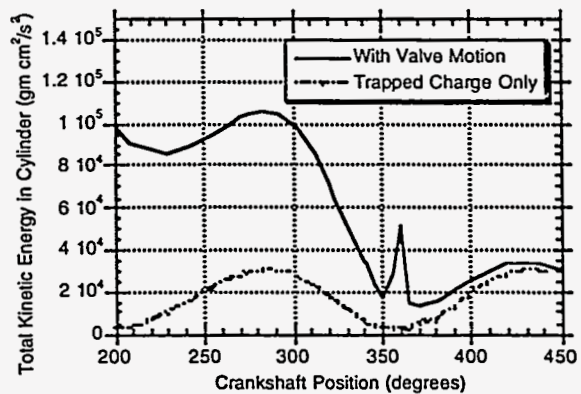


Fig. 9 - Total bulk-flow kinetic energy history averaged over the cylinder.

the fast burn combustion case, due to the higher temperatures.

The large difference in the combustion rate and NO_x emissions in the two simulations illustrate the importance of modeling the bulk flow and turbulence levels accurately. In Figs. 9 and 10 are plotted the total kinetic energy of the bulk flow and the turbulent kinetic energy as modeled by the k-ε turbulence model. These curves show a significant difference in the initial kinetic energy levels of the two simulations. As the initial high kinetic energy level dissipates in the induction run and as the piston adds kinetic energy during compression, the averaged kinetic energy for both the bulk flow and turbulence of the quiescent run are within 32-40 percent of air induction run at ignition (346 CA). Because the flame speed is proportional to the turbulent kinetic energy, the observed

flame speed should differ by 40 percent if the averaged kinetic energy values represented the values near the combustion front. Instead, a factor of 350 percent is observed. This is strong evidence that the flow has a non-uniform turbulence distribution and is sensitive to the details of the flow history.

Engine CFD modeling summary

A computational mesh was created of the SNL Onan engine, with an accurate description of the intake and exhaust valves. In the absence of experimental data on the performance of the engine, we focused on observed trends in the simulations. The model of the Onan engine was used to investigate the induction process of fresh charge and the subsequent compression and combustion of hydrogen with NO_x formation. A major

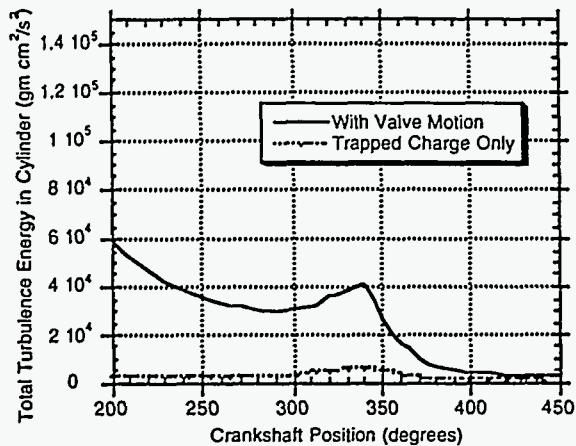


Fig. 10 - Total turbulent kinetic energy history averaged over the cylinder.

conclusion of the investigation is that the use of a single kinetic reaction for hydrogen oxidation is unable to describe both the observed laminar flame speed and the lack of autoignition in the Onan engine. We also observed that the combustion and emissions are sensitive to the initial flow field at the beginning of combustion. NO_x emissions were observed to vary by a factor of 2 with typical choices for the initial conditions of the simulation. We conclude that any modeling of the Onan engine must include the effects of the intake flow on the bulk flow and turbulence levels during combustion.

The KIVA-3 simulations are now at the ideal stage of development to begin the validation process as the experimental data become available from Sandia Combustion Research Facility. The observed sensitivity of hydrogen combustion to turbulence and bulk flow, highlights the need for improved kinetics and then for validation of the kinetics in conjunction with the mixing controlled models. In addition, as experimental data for the Onan engine becomes available, the simulation conditions can be improved to better model the experiments. For example, the constant pressure boundary conditions can be replaced by time-varying pressure boundary conditions as determined from the experiments. The pressure history and the mass of charge in the engine can then be compared to the experimental results to further validate the performance of the valve model in KIVA-3. Finally, comparison of NO_x formation and engine efficiencies will be made. Once the simulations are validated, an analysis of the operation of the engine will be undertaken to better understand the experimental observations of the effect of combustion

chamber geometry, turbulence levels, flame speed, and heat transfer on NO_x formation and efficiency. The simulations can also be used to suggest modifications to the Onan engine experiment to improve the performance and reproducibility of the engine. For example, the trends in the present report suggest that a reduction in the turbulence levels of the engine through the introduction of shrouds on the valves may reduce NO_x emissions. This is an ideal application of using computer simulations to improve the success of expensive modifications of an experiment.

ENGINE DESIGN SUMMARY

Six requirements have been identified as important in obtaining a high efficiency engine that can be used in a hybrid series vehicle that approaches the 34 km/l (80 mpg) PNGV goal 3. These requirements suggest the use of a very lean hydrogen engine with a high compression ratio and long stroke. We have used both a simplified engine model and an advanced CFD model to predict trends in engine performance characteristics. The results indicate that a 1.8 liter engine operating with hydrogen at an equivalence ratio of 0.4 and 1800 RPM will have an estimated output of 15 kW with a thermal efficiency of 45%. Supercharging and increasing engine speed results in the 40-45 kW of power necessary for long hill climbs. An ongoing experimental evaluation of a preliminary engine design based on an Onan engine will be used to validate the hydrogen combustion model in KIVA-3 which will be applied to the proposed new engine geometry.

ACKNOWLEDGEMENTS

This work was performed under the auspices of the U.S. Department of Energy by the Lawrence Livermore National Laboratory under Contract No. W-7405-ENG-48 and by Los Alamos National Laboratory under Contract No. W-7405-ENG-36.

REFERENCES

- Aceves, S. M., and Smith, J. R., 1995, "A Hybrid Vehicle Evaluation Code and Its Application to Vehicle Design," SAE paper 950491.
- Alkidas, A. C. and Suh, I., 1991, "The Effects of Intake-Flow Configuration on the Heat-Release and Heat-Transfer Characteristics of a Single-Cylinder Four-Valve S.I. Engine," SAE paper 910296.
- Amsden, A. A., 1993, "KIVA-3: A KIVA Program with Block Structured Mesh for Complex Geometries," Los Alamos National Laboratory report LA-12503-MS.
- Amsden, A. A., Butler, T. D., and O'Rourke, P. J., 1989, "KIVA-II: A Computer Program for Chemically Reactive Flows with Sprays," Los Alamos National Laboratory report LA-

11560-MS.

Abdel-Gayed, R. G. and Bradley, D., 1977, "Dependence of Turbulent Burning Velocity on Turbulent Reynolds Number and Ratio of Laminar Burning Velocity to RMS Turbulent Velocity," Sixteenth Symposium on Combustion, The Combustion Institute, p. 1725.

Barnes-Moss, H.W., 1975, "A Designer's Viewpoint," Passenger Car Engines Conference Proceedings, Institution of Mechanical Engineers, London, pp. 133-147.

Johnson, N. L., Amsden, A. A., Naber, J. D., Siebers, D. L., "Three-dimensional Computer Modeling of Hydrogen Injection and Combustion," Transaction paper for the '95 High Performance Computing Conference, edited by Adrian Tentner. pp. 61-69. Published by the Society for Computer Simulation, 1995.

Magnussen, B. F. and Hjertager, B. H., 1977, Sixteenth Symposium on Combustion, The Combustion Institute, pp. 719-729.

Meier, F., Kihler, J., Stolz, W., Bloss, W. H. and Al-Garni, M., 1994, "Cycle Resolved Hydrogen Flame Speed Measurements with High Speed Schlieren in a Hydrogen Direct Injection SI Engine," SAE Fuels and Lubricants Meeting and Expositions, SAE paper 942036.

Muranaka, S., Takagi, Y. and Ishida, T., 1987, "Factors Limiting the Improvement in Thermal Efficiency of S. I. Engine at Higher Compression Ratio," Society of Automotive Engineers Transactions, SAE paper 870548.

Oehmichen, M., 1942, "Hydrogen as an Engine Fuel," Engine Laboratory of the Technische Hochschule, Dresden,

Germany, VDI-Verlag GmbH, Berlin NW, V.D.I. Paper No. 68.

Olsson, K., and Johansson, B., 1995, "Combustion Chambers for National Gas SI Engines Part II: Combustion and Emissions," SAE paper 950517.

Ross, M., and Wu, W., 1995, "Fuel Economy Analysis for a Hybrid Concept Car Based on a Buffered Fuel-Engine Operating at an Optimal Point," SAE paper 950958.

Smith, J. R., 1994, "Optimized Hydrogen Piston Engines." SAE Convergence '94, Detroit, MI., Oct 1994.

Smith, J. R., Aceves, S. M. and Van Blarigan, P., 1995, "Series Hybrid Vehicles and Optimized Hydrogen Engine Design," submitted for presentation at 1995 SAE Future Transportation Technology Conference, Costa, Mesa, CA, Aug 7-10, 1995.

Van Blarigan, P., 1995, "Hydrogen Hybrid Vehicle Engine Development: Experimental Program," Sandia National Laboratory, Proceedings of the 1995 DOE Hydrogen Program Review, April 1995.

Watts, P. A. and Heywood, J. B., 1980, "Simulation Studies of the Effects of Turbocharging and Reduced Heat Transfer on Spark-Ignition Engine Operation," SAE paper 800289.

Westbrook, C. K., personal communication. September 1994

Woschni, G., 1967, "Universally Applicable Equation for the Instantaneous Heat Transfer Coefficient in the Internal Combustion Engine," SAE paper 670931, SAE Transactions, Vol. 76.